ACS Sustainable Chemistry & Engineering

pubs.acs.org/journal/ascecg

Research Article

Green Electrospinning of Chitosan/Pectin Nanofibrous Films by the Incorporation of Cyclodextrin/Curcumin Inclusion Complexes: pH-Responsive Release and Hydrogel Features

Asli Celebioglu,* Antonio Frank Saporito, and Tamer Uyar*

Cite This: ACS Sustainable Chem. Eng. 2022, 10, 4758−4769

Read Online

ACCESS | Metrics & More | Article Recommendations | Supporting Information

ABSTRACT: Chitosan and pectin are abundantly found biopolymers in nature that are derived from renewable resources. On the other hand, the chemical structure of these biopolymers creates problems during the production of their nanofibrous films by the electrospinning technique. In this study, the electrospinning of the chitosan/pectin blend system was facilitated using natural, starch-derived cyclodextrin (hydroxypropyl-γ-cyclodextrin (HPγCD)) molecules and nanofibrous films were generated with a green approach in which there was no use of a carrier polymer or toxic solvent. The nanofibrous films obtained with different chitosan/pectin ratios showed high swelling (water uptake) property (~1340 to 1510%), which suggested the hydrogel-forming capacity of these electrospun films. Here, the HPγCD molecules were further utilized and curcumin, a well-known bioactive compound, was encapsulated into HPγCD cavities by inclusion complexation. This time, HPγCD−curcumin inclusion complexes (ICs) were mixed with chitosan/pectin blends using the predetermined ratios, and freestanding nanofibrous films were successfully produced having an ~89% curcumin loading efficiency. The ultimate nanofibrous films demonstrated a pH-responsive release profile of curcumin in pH 5.4 and 7.4 media besides their high swelling feature. Briefly, chitosan/pectin/CD-IC nanofibrous films can be a promising alternative to biomaterials produced with synthetic sources by holding the unique properties of biopolymers, CD, and nanofibers.

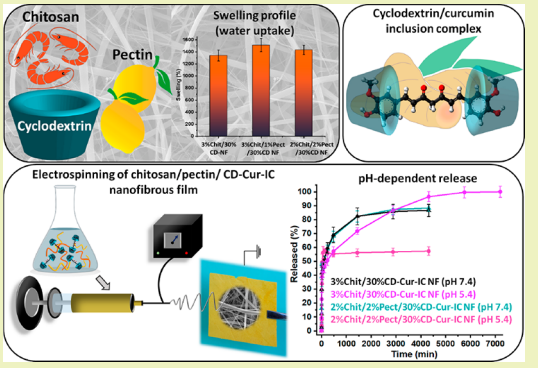

KEYWORDS: *green electrospinning, cyclodextrin, biopolymers, chitosan, curcumin, hydrogel nanofibers, pH-responsive release*

INTRODUCTION

The development and manufacturing of biobased products is a weighty matter of today's world due to the disastrous consequences of the ever-growing consumption of nonrenewal fossil-based resources.[1,2] The production of biomaterials based on eco-friendly sources has indeed become a cruciality to remove the destructive impact of petroleum-based products on the environment.[1,2] A large number of biopolymers from natural and renewable sources have been recently positioned for various purposes in biomedical, pharmaceutical, environmental, food, and agricultural areas due to their biocompatibility, biodegradability, and low toxicity.[3] Herein, natural biopolymers, polysaccharides have risen to prominence among others by possessing a wide range of mechanical and physicochemical properties. Polysaccharides are one of the most abundantly found biopolymer types, which can be acquired from plants, animals, and microorganisms.[4] As a well-known polysaccharide, chitosan is a sustainable raw material obtained by partial deacetylation of chitin that can be extracted from the exoskeletons of arthropods.[5] Pectin is also another abundantly found polysaccharide type that can be extracted from the citrus peel, sugar beet pulp, and apple pomace.[6] In other words, both chitosan and pectin can render the utilization from the residuals of industrial activities possible. These biopolymers have been already used as gelling, thickening, filling, or emulsifying agents in the pharmaceutical and food industries.[4−6] However, the conversion of these renewable biopolymer sources into high added-value products can be one of the main breakthroughs of their sustainability.

Chitosan consists of randomly distributed β-(1−4)-linked D-glucosamine (deacetylated) and *N*-acetyl-D-glucosamine (acetylated) units. On the other hand, pectin includes (1 → 4)-α-D-galacturonic acid residues branched with different neutral sugars (Figure 1a).[5,6] The chemical composition of these polysaccharides establishes their functionalities for potential biomedical and pharmaceutical applications.[5,6] The unique cationic nature of chitosan and the adjustable ionic structure of pectin under different pH conditions ensure biological

Received: January 31, 2022
Revised: March 18, 2022
Published: March 30, 2022

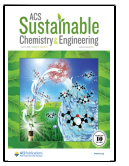

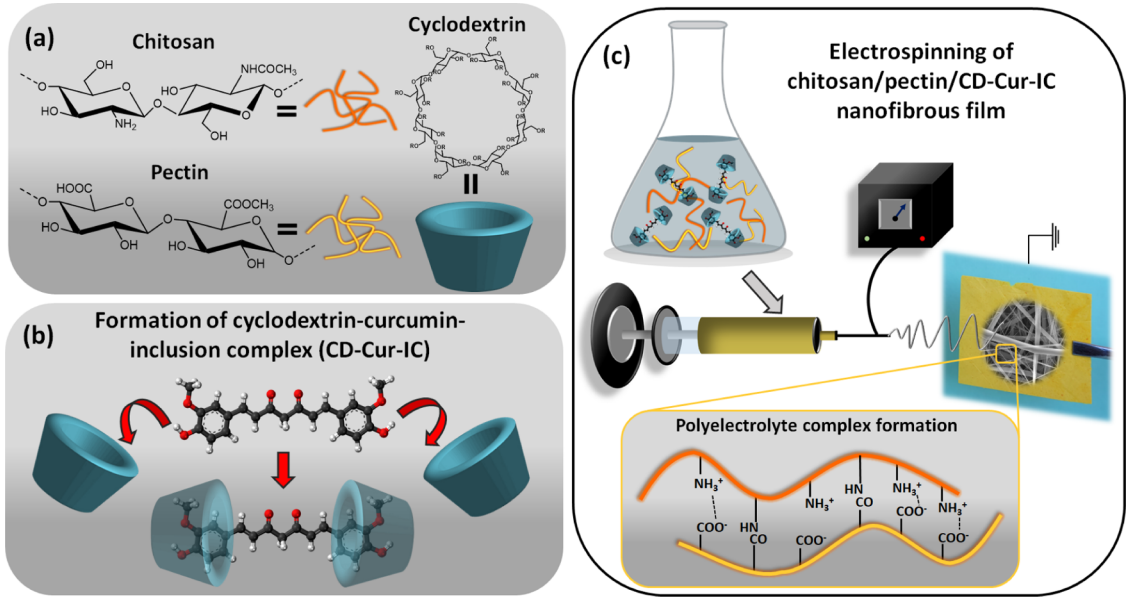

Figure 1. (a) Chemical structure of chitosan, pectin, and hydroxypropyl-γ-cyclodextrin (R: −H or $-CH_2CHOHCH_3$). (b) The schematic representation of inclusion complex (IC) formation between cyclodextrin (CD) and curcumin (Cur). (c) The schematic representation of the electrospinning of the chitosan/pectin/CD−Cur-IC nanofibrous film.

activities including antimicrobial, antioxidant, antifungal, and antitumor, along with particular physicochemical properties such as forming hydrogels.[5,6] Accordingly, the use of chitosan and pectin in the form of nanofibrous films might suggest a powerful platform that combines the high surface area, porosity, flexibility, and lightweight features of nanofibers with the inherent benefits of these biopolymers. The high swelling (water uptake) property of these biopolymers may even enable the generation of hydrogel nanofiber systems, which is recently quite attractive for wound healing applications.[7,8]

Electrospinning is one of the simplest and most promising ways of generating nanofibrous films from a variety of polymers that also facilitate the simultaneous encapsulation of different types of active compounds with high efficiency for various application purposes.[9−13] On the other hand, there is a challenge arising out of the chemical structures of chitosan and pectin and creating trouble during their electrospinning. Here, the branchy, rigid, and ionic structure of chitosan and pectin can impede the preparation of electrospinning solutions having the proper level of viscosity and electrical charges, which are essential to ensure jet stability during the process for the uniform fiber formation.[4,14−16] Moreover, derivation of these biopolymers from different batches of natural sources can adversely affect the reproducibility of the process. As a typical approach, chitosan and pectin have been blended with the other carrier polymers such as poly(ethylene oxide) (PEO), poly(vinyl alcohol) (PVA), poly(ethylene terephthalate) (PET), polycaprolactone (PCL), poly(lactic acid) (PLA), zein, and gelatin to be electrospun into freestanding nanofibrous films.[4,14−17] Here, the solvent type used for the electrospinning of nanofibers has been chosen properly for the carrier polymer types in general. To the best of our knowledge, there has been no reported study in the literature about the electrospinning of neat pectin nanofibers. On the other hand, the neat chitosan nanofibers have been generated without using a carrier polymeric matrix.[15,17,18] In these related studies where pure chitosan was electrospun into nanofibers, the highly toxic and corrosive solvent trifluoroacetic acid (TFA) and its mixture with dichloromethane (DCM) were found to be the most proper solvent systems for the efficient electrospinning of neat chitosan nanofibers.[15,17,18] Development of alternative and "green" ways for the electrospinning of these two biopolymer types would be particularly attractive and essential for promoting their biomedical administration. In one of the related studies, Burns et al. have earlier reported the use of small molecules, cyclodextrins, to facilitate the fiber formation of chitosan in an acetic acid solution instead of using an additional carrier polymer.[19]

As a type of oligosaccharides, cyclodextrins (CDs) have drawn great attention of the global market of pharmaceutical and food trades.[20,21] Since they are classified as Generally Recognized as Safe (GRAS) by the U.S. Food and Drug Administration, they have been already widely used in the formulation of drugs. These starch-derived molecules can form noncovalent interactions with a variety of active agents, and this makes them the main source of attention as an encapsulation agent. As a result of inclusion complexation with CD, the aqueous solubility, stability, and bioavailability of bioactive compounds can be enhanced noticeably.[20,21] Even the highly water-soluble hydroxypropylated derivative of CDs and their inclusion complexes can be electrospun into freestanding nanofibrous films without using an additional polymeric matrix or toxic chemicals.[22−27] In this study, highly water-soluble hydroxypropyl-γ-CD (HPγCD) (>500 mg/mL) was used as a carrier matrix to generate nanofibrous films from chitosan and chitosan/pectin blend systems. HPγCD is a hydroxypropylated version of native γCD, and it has been approved by the U.S. Food and Drug Administration (FDA) as an inert excipient that can be used in topical products.[28] Here, nanofibrous films were prepared with different ratios of biopolymers to evaluate the potential polyelectrolyte complex formation between the polar functional groups of chitosan and pectin by intermolecular interaction. Afterward, HPγCD/curcumin inclusion complexes were generated and then mixed with the chitosan/pectin blends using the determined

https://doi.org/10.1021/acssuschemeng.2c00650
ACS Sustainable Chem. Eng. 2022, 10, 4758−4769

polymer ratios for the further pH-responsive release analysis (Figure 1b,c). Curcumin is a well-known bioactive compound that is extracted from the rhizome of turmeric (Curcuma longa) and holds numerous pronounced properties including anti-inflammatory, antimicrobial, antidiabetic, antioxidant, etc.[29] CD inclusion complexation is one of the most effective ways to improve the aqueous solubility, and so the bioavailability of this non-water-soluble active compound and HPγCD was chosen depending on our previous results in which HPγCD provided significantly higher aqueous solubility compared to other hydroxypropylated derivatives of βCD.[25] Briefly, we have adopted a green approach in which high-valued nanofibrous biomaterials were obtained using completely sustainable and biocompatible sources of chitosan, pectin, cyclodextrin, and curcumin. This approach does not involve toxic chemicals or processes to reach the pH-responsive and hydrogel formation features, which suggest the high potential to be used in biomedical applications.

EXPERIMENTAL METHODS

Materials. Hydroxypropyl-γ-cyclodextrin (HPγCD) (Cavasol W8 HP, DS: ∼0.6) was kindly gifted by Wacker Chemie AG for scientific research. Chitosan, (85% deacetylated, MW 300,000−500,000 g/mol, Alfa Aesar), pectin citrus (Alfa Aesar), curcumin (≥98%, Acros Organics), acetic acid (Glacial, GR, ACS, Merck), dimethyl sulfoxide (DMSO, >99.9%, Sigma-Aldrich), phosphate-buffered saline tablet (Sigma-Aldrich), sodium acetate (anhydrous, ACS, 99%, Alfa Aesar), and deuterated dimethyl sulfoxide (d_6-DMSO, 99.8%, Cambridge Isotope) were used as received. High-quality distilled water was provided by Millipore Milli-Q ultrapure water system (Millipore).

Preparation of the Solutions for Electrospinning. The electrospinning systems were prepared to have different combinations (%, w/v (with respect to solvent volume)) of polymers (chitosan and pectin) and HPγCD. From this point on, HPγCD will be called with the abbreviation of CD in case of sample naming. The clear solutions of chitosan (3%), chitosan (3%)/pectin (1%), chitosan (2%)/pectin (2%), chitosan (2%)/pectin (2%)/CD (20%), chitosan (3%)/CD (30%), chitosan (3%)/pectin (1%)/CD (30%), and chitosan (2%)/pectin (2%)/CD (30%) were prepared in the solvent mixture of acetic acid/water (9/1, v/v). The solution properties of viscosity and conductivity were verified for each system using a rheometer (AR 2000 rheometer, TA Instruments) (cone/plate spindle (20 mm diameter and 4° cone angle), shear rate range: 0.01−1000 s^{-1} (21 °C)) and a conductivity-meter (FiveEasy, Mettler Toledo), respectively. Afterward, electrospinning equipment (Spingenix, model: SG100, Palo Alto) was employed to produce nanofibrous films. For this, each solution was loaded in a plastic disposable syringe fixed with the metallic nozzle (21 G) and fed through this nozzle with a flow rate of 0.5 mL/h. A high voltage (15 kV) was applied to the nozzle for the formation and deposition of nanofibers on the stationary metal collector (15 cm away from the nozzle) as a film. The freestanding nanofibrous film was efficiently obtained at ambient conditions recorded to be 20 °C with a relative humidity of 35%.

On the other hand, the inclusion complex of curcumin and HPγCD was synthesized using the freeze-drying method. For this, curcumin and HPγCD having a molar ratio of 4:1 (CD/guest) was stirred at 50 °C for 24 h. Afterward, the mixture was frozen at −20 °C and then kept in a freeze-dryer for 2 days to obtain powder form of HPγCD−curcumin inclusion complexes (CD−Cur-IC). For control, CD−Cur physical mixture (PM) was also prepared using the same molar ratio of 4:1 (CD/guest) by blending two components until a homogeneous mixture was obtained. The CD−Cur-IC was incorporated into chitosan (3%)/pectin (1%) and chitosan (2%)/pectin (2%) systems with 30% (w/v) just like pure HPγCD. First, polymers were dissolved in acetic acid/water (9/1, v/v) and then CD−Cur-IC powder was dispersed in these polymer solutions at room temperature. For control, the curcumin powder was also mixed into clear solutions of chitosan (3%)/pectin (1%)/CD (30%) and chitosan (2%)/pectin (2%)/CD (30%) systems for following the effect of incorporation of the inclusion complex on electrospinning. Electrospinning of the curcumin-included system was also conducted using the same protocol as mentioned above. All collected nanofibrous films were thermally treated at 120 °C for 1 h.

Morphological Analysis. The morphology of nanofibrous films was examined using a scanning electron microscope (SEM, Tescan MIRA3, Czech Republic). Prior to the measurements, samples were fixed on the SEM stubs and sputtered with the thin layer of Au/Pd to moderate the charging problem. SEM imaging was performed under high vacuum by applying an accelerating voltage of 10 kV and with a working distance of 10 mm. The average diameter (AD) of nanofibers (n = ∼100) was verified by ImageJ software and given as average diameter ± standard deviation.

Structural Analyses. An attenuated total reflectance Fourier transform infrared (ATR-FTIR) spectrometer (PerkinElmer) was used to record the FTIR spectra of samples. Each spectrum was obtained in the range of 4000−600 cm^{-1} upon 32 scans at a resolution of 4 cm^{-1}. A thermogravimetric analyzer (TGA, Q500, TA Instruments) was operated to evaluate the thermal profile of the samples. A heating rate of 20 °C/min was used to increase the temperature from room temperature to 600 °C under the inert atmosphere (N_2).

The powder CD−Cur-IC was additionally analyzed using further techniques. The X-ray diffraction patterns of curcumin, HPγCD, CD−Cur-IC, and CD−Cur-PM were identified by an X-ray diffractometer (XRD, Bruker D8 Advance ECO). The XRD graphs were recorded in the range of 2Θ = 5−30° by Cu Kα radiation (40 kV and 25 mA). The thermal profile of curcumin, HPγCD, CD−Cur-IC, and CD−Cur-PM was also checked using a differential scanning calorimeter (DSC, Q2000, TA Instruments). The samples placed in the Tzero aluminum pan were heated using a heating rate of 10 °C/min from 0 to 240 °C (N_2). A nuclear magnetic resonance spectrometer (Bruker AV500 with autosampler) was used to calculate the molar ratio of CD−Cur-IC. For this, the powder forms of curcumin, HPγCD, and CD−Cur-IC were dissolved in d_6-DMSO at a sample concentration of 70 g/L. The proton nuclear magnetic resonance (^{1}H-NMR) spectra were obtained upon 16 scans, and Mestranova software was run to calculate the integration of chemical shifts (δ, ppm). The molar ratio (CD/guest) of CD−Cur-IC powder was calculated taking into account the $-CH_3$ peak of HPγCD at 1.03 ppm and protons of curcumin between 6.50 and 8.00 ppm.

Disintegration, Swelling, and Degradation Tests. For dissolution test, the thermally treated and nontreated nanofibrous films of chitosan (3%)/CD (30%), chitosan (3%)/pectin (1%)/CD (30%), and chitosan (2%)/pectin (2%)/CD (30%) having a dimension of ∼1.5 cm × 1.5 cm were located into plastic Petri dishes and then 3 mL of water was poured onto samples. A video was recorded at the same time to follow the disintegration profile of samples (Videos S1−S3). The degradation and the swelling profiles of the thermally treated nanofibrous films were examined using the PBS (pH 7.4) and acetate (pH 5.4) buffer media at 37 °C. First, ∼4 mg of sample was immersed in 4 mL of buffers and shaken on the incubator shaker for 24 h at 37 °C. Afterward, swollen nanofibrous films were taken from the liquid medium and weighted using analytic balance after removing the excess amount of liquid medium from the surface of the samples. For degradation profile, the samples swollen in buffers were placed in the fume hood to dry till they reached a stable weight. The swelling degree (%) and degradation degree (%) of each sample were calculated by the following formulas

$$\text{swelling degree (\%)} = (W - W_0)/W_0 \times 100 \quad (1)$$

$$\text{degradation degree (\%)} = W_i/W_0 \times 100 \quad (2)$$

where W_i, W_0, and W are the weight of initial, dried, and swollen nanofibrous films, respectively.

Loading Efficiency Test. Since nanofibrous films of 3%Chit/30% CD−Cur-IC and 2%Chit/2%Pect/30%CD−Cur-IC are not being completely dissolved in solvent systems, samples were immersed in

https://doi.org/10.1021/acssuschemeng.2c00650
ACS Sustainable Chem. Eng. 2022, 10, 4758−4769

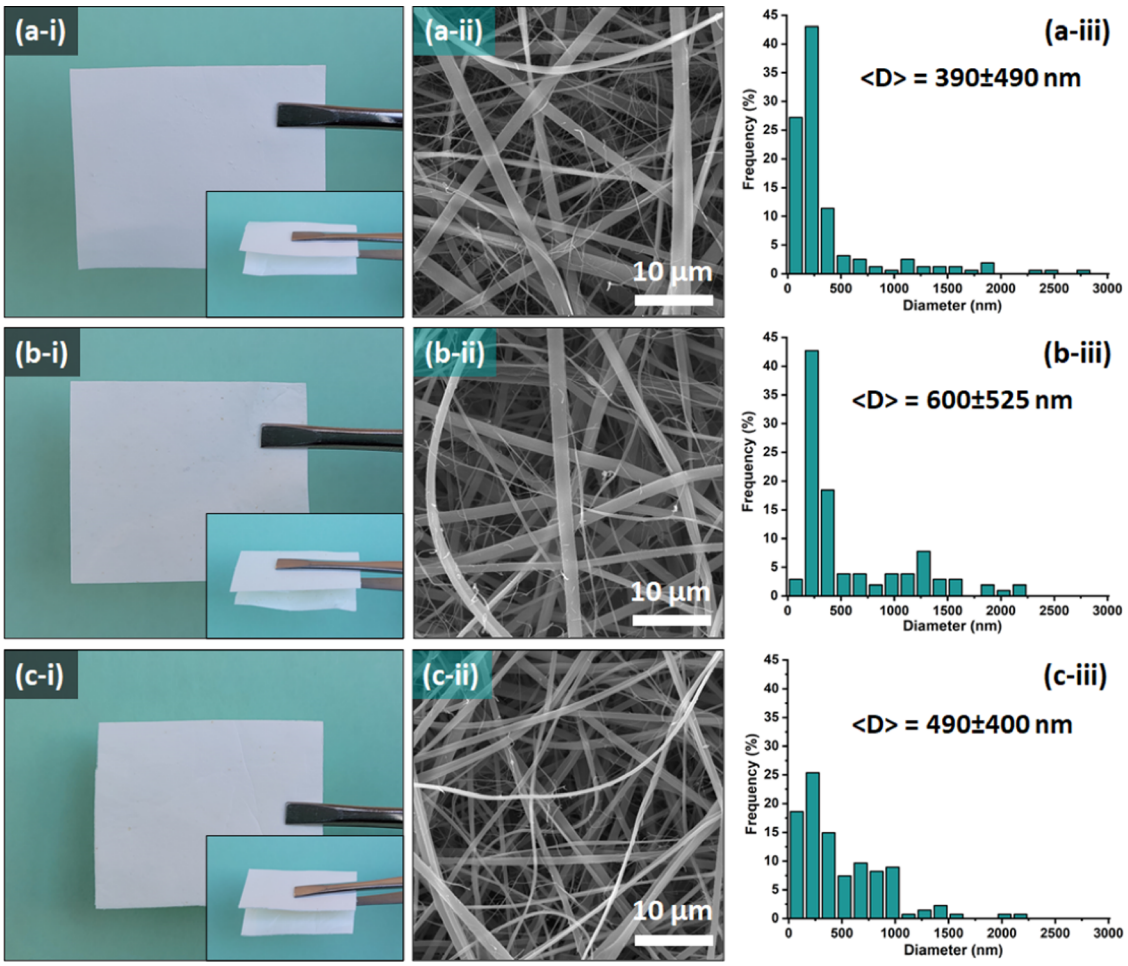

Figure 2. (i) Photos, (ii) SEM images, and (iii) fiber diameter distributions of (a) 3%Chit/30%CD NF, (b) 3%Chit/1%Pect/30%CD NF, and (c) 2%Chit/2%Pect/30%CD NF after thermal treatment.

dimethyl sulfoxide (DMSO) to extract curcumin molecules from samples. The loading efficiency value was determined by ultraviolet−visible (UV−vis) spectroscopy (PerkinElmer, Lambda 35) measurements (435 nm) of extraction aliquots. The calibration curve of curcumin in DMSO indicated acceptability with $R^2 \geq 0.99$. Three replications were performed for each sample, and the results were given as mean values ± standard deviations. The following formula was used to calculate the loading efficiency (%)

$$\text{loading efficiency (\%)} = \text{Ce/Ct} \times 100 \quad (3)$$

where Ce and Ct are the concentration of the loaded curcumin and the initial concentration of curcumin, respectively.

***In Vitro* Release Test.** The time-dependent release test of 3% Chit/30%CD−Cur-IC and 2%Chit/2%Pect/30%CD−Cur-IC nanofibrous films was conducted in two different liquid media having pH values of 7.4 and 5.4. For this, 10 mg of sample was immersed in 10 mL of buffer/ethanol (7/3, v/v) system at 37 °C. While the systems were being shaken on the incubator shaker at 150 rpm, 0.75 mL of aliquot was withdrawn and the fresh one was readded to the systems at certain time intervals. The UV−vis spectroscopy measurements (430 nm) were carried out to verify the amount of curcumin released from nanofibrous films. The calibration curve of curcumin in buffer solutions showed $R^2 \geq 0.99$ linearity, and the amount of curcumin released was calculated by converting the absorbance intensity of aliquots into %. Triplicate tests were performed for each sample (mean values ± standard deviations), and release kinetics were examined using different kinetic models (see the Supporting Information).

Statistical Analyses. The statistical analyses were performed using the one-way/two-way analysis of variance followed by Tukey's test (ANOVA). OriginLab (Origin 2021) was used for all of these ANOVA tests (0.05 level of probability).

RESULTS AND DISCUSSION

Morphology of Nanofibrous Films. Electrospinning conducted in the absence of HPγCD revealed no fiber formation for all three systems including 3%Chit, 3%Chit/1%Pect (w/v), and 2%Chit/2%Pect (w/v) (Figure S1a−c). On the other hand, the same polymeric systems were electrospun into homogeneous nanofibers by the addition of HPγCD (Figure 2). This finding revealed that HPγCD enhanced the fiber formation from chitosan and pectin solutions. Here, the beaded nanofibers were obtained with a lower HPγCD content of 20% (w/v) for the 2%Chit/2%Pect (w/v) system (Figure S1d). Therefore, the HPγCD concentration was increased to 30% (w/v) for generating uniform nanofiber structures. The comparable finding has also been reported by Burns et al. in one of the related studies where the electrospinnability of chitosan in acetic solution was improved with the HPβCD addition.[19] In this related study, it has been indicated by the systematic rheological measurements that HPβCD promoted the association and entanglement of chitosan polymer chains in the electrospinning solution, which is essential to form nanofibers.[19] Here, the addition of 30% of HPγCD (w/v) facilitated the electrospinning of all

https://doi.org/10.1021/acssuschemeng.2c00650
ACS Sustainable Chem. Eng. 2022, 10, 4758−4769

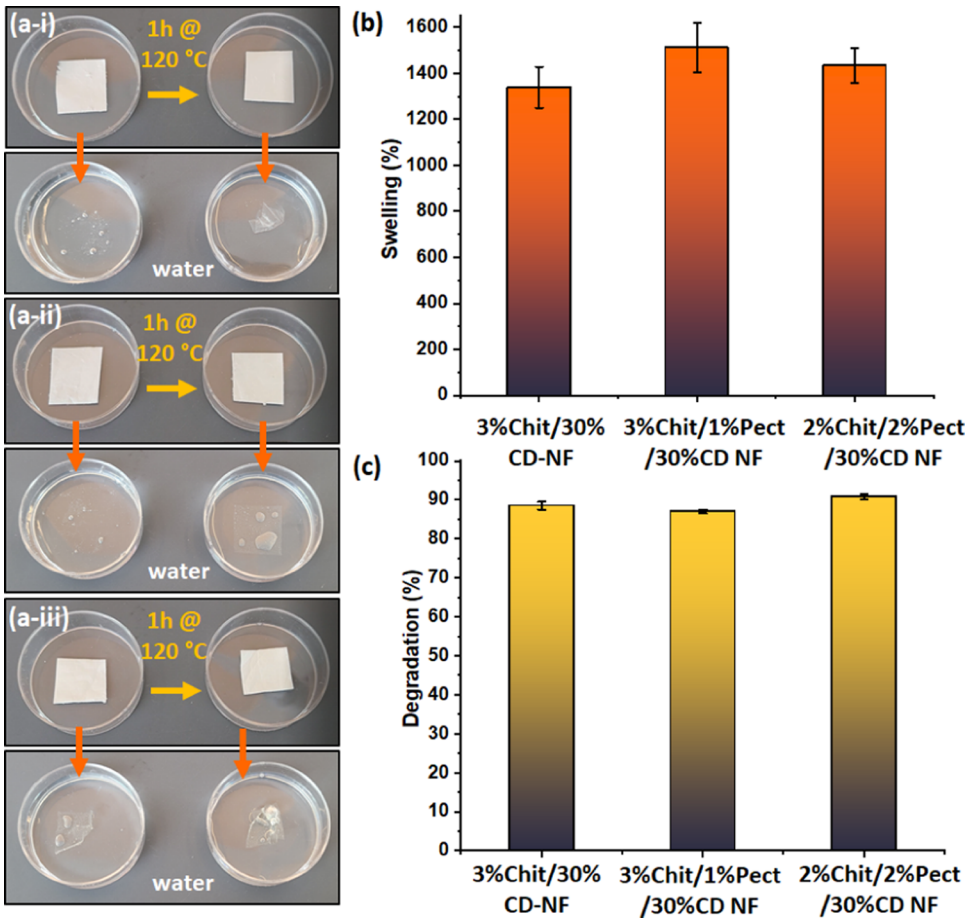

Figure 3. (a) Disintegration profile of (i) 3%Chit/30%CD (BT) NF and 3%Chit/30%CD NF. (ii) 3%Chit/1%Pect/30%CD (BT) NF and 3% Chit/1%Pect/30%CD NF, and (iii) 2%Chit/2%Pect/30%CD (BT) NF and 2%Chit/2%Pect/30%CD NF. (b) Swelling and (c) degradation profile of 3%Chit/30%CD NF, 3%Chit/1%Pect/30%CD NF, and 2%Chit/2%Pect/30%CD NF.

three systems; 3%Chit, 3%Chit/1%Pect, 2%Chit/2%Pect, and freestanding nanofibrous films (NFs) were obtained having mechanical integrity (Figure 2a,b,c-i). SEM images of 3%Chit/30%CD NF, 3%Chit/1%Pect/30%CD NF, and 2%Chit/2% Pect/30%CD NF showed the homogeneous fiber formation with no observable defects (Figure 2a,b,c-ii). The respective average fiber diameter (AFD) was 390 ± 490, 600 ± 525, and 490 ± 400 nm for 3%Chit/30%CD NF, 3%Chit/1%Pect/30% CD NF, and 2%Chit/2%Pect/30%CD NF, respectively (Figure 2a,b,c-iii). The results of statistical calculations showed that the mean diameter of 3%Chit/1%Pect/30%CD NF is significantly different from that of 3%Chit/30%CD NF ($p < 0.05$), while the mean diameter of 2%Chit/2%Pect/30%CD NF has no significant differences compared to the other two samples ($p > 0.05$).

Here, enhancing the electrospinning of chitosan and chitosan/pectin blend into freestanding nanofibrous films by the incorporation of HPγCD was clarified by the viscosity and conductivity measurements.[9,30] Table S1 summarizes findings of the viscosity and conductivity measurements. For the HPγCD-free systems, the conductivity of solutions was found to be at around ∼450 μS/cm, and the viscosity values were, respectively, detected at ∼0.5 and ∼0.2 Pa·s for 3 and 2% (w/v) chitosan concentrations. It is obvious that the chitosan concentration is quite influential on the viscosity of the solutions due to its high molecular weight (M_W 300,000−500,000 g/mol). By the addition of 20% (w/v) HPγCD in the solution, the viscosity values increased to 0.462 from 0.209 Pa·s for 2% chitosan/2% pectin-based system, while conductivity decreased from 453.1 to 168.6 μS/cm (Table S1). These variations enabled the partial stretching of the electrospinning jet into beaded fiber structures (Figure S1d). For each system, 30% (w/v) HPγCD content in the solutions provided the essential higher viscosity and lower conductivity values that ensured a stabilized stretching for the jet and so uniform fiber formation.[9] Here, the enhanced viscosity contributed to the association of polymer chains by initiating the higher degree of entanglement that is crucial for fiber formation. The increase of solution viscosity values by the addition of CD can be principally considered quite enough to reach the required stretching during the electrospinning process. However, solution conductivity is the other most prominent element influencing the morphology of samples.[9] Such that, the highly conductive solutions can deplete the electrostatic repulsion since the surface charges cannot be collected on the jet and this can lead to trouble during the Taylor cone formation.[9] Therefore, the conductivity of solution also needs to be in the proper range to generate uniform nanofibers. Based on this, the diminishing of the solution conductivity values from ∼450 to ∼100 μS/cm ranges by the addition of CD might have eliminated the jet instabilities, which increased from the highly charged nature of chitosan and pectin in acetic solution.

Structural Analyses of Nanofibrous Films. Fourier transform infrared (FTIR) spectra are given in Figure S2. For

https://doi.org/10.1021/acssuschemeng.2c00650
ACS Sustainable Chem. Eng. 2022, 10, 4758−4769

the FTIR spectrum of HPγCD, the absorption band at 1645 cm^{-1} is attributed to H−O−H deformation.[31] On the other hand, chitosan has the C═O stretching vibration of amide I at 1648 cm^{-1} and the NH bending of amide II at 1590 cm^{-1}.[32] The shifting of the absorption band of chitosan from 1590 cm^{-1} to a lower frequency (1564 cm^{-1}) is evidence for the electrostatic interaction between the hydroxyl groups of HPγCD and $-NH_3^+$ of chitosan in 3%Chit/30%CD NF before thermal treatment.[33] After the thermal treatment at 120 °C for 1 h, the pattern of the same region further changed and the peak at 1564 cm^{-1} was lost, while the peak at 1645 cm^{-1} increased in strength (Figure S2a). This can be associated with the dehydration reaction, which might have led to the formation of stronger interaction between HPγCD and chitosan.[34] In the FTIR spectra of pectin, the absorption bands related to the carboxyl group and C═O stretching of the methyl ester group are, respectively, observed at 1623 and 1734 cm^{-1} (Figure S2b,c).[32] By the addition of pectin, the peak at 1564 cm^{-1} was diminished and a broader shoulder appeared at the similar region of the spectrum (1595−1525 cm^{-1}) of thermally untreated 3%Chit/1%Pect/30%CD NF and 2%Chit/2%Pect/30%CD NF. This is evidence of the polyelectrolyte complex formation by more favorable and effective ionic interaction between positively charged amino groups of chitosan and negatively charged carboxyl groups of pectin compared to that occurred in the case of the HPγCD only.[32] After the thermal treatment, a similar pattern was observed in pectin-included NF (Figure S2b,c) like the pectin-free one (Figure S2a) with the increasing strength of the 1650 cm^{-1} peak and the loss of the shoulder at 1595−1525 cm^{-1}. This is due to the partial formation of an amide-type bond between pectin and chitosan in addition to the potential interaction that occurred between HPγCD and chitosan within the sample structure.[34,35] Even in the related study of Bernabé et al., it was revealed that the thermal treatment of the pectin/chitosan membrane enabled us to obtain insoluble membranes by the conversion of $-NH_3^+$ $^-$OOC− ionic bonds into amide bonds.[35] On the other hand, the peak at 1734 cm^{-1} corresponded to the methyl ester group of pectin was kept on observing in the spectrum with increasing intensity for 2% Chit/2%Pect/30%CD NF (Figure S2c) compared to that for 3%Chit/1%Pect/30%CD one (Figure S2b). This demonstrated that the ester group did not take place in the interactions in the sample.[36]

The TGA thermograms of HPγCD, chitosan, and NF before and after thermal treatment are given in Figure S3 with their derivatives (DTG). In the case of pristine HPγCD and chitosan, there are two main weight losses: (i) the dehydration of water until ∼130 °C and (ii) the main degradation of HPγCD and chitosan at 351 and 300 °C, respectively. On the other hand, the DTG of 3%Chit/30%CD NF reduced in intensity, became wider, and shifted slightly to the lower temperature (348 °C) compared to pristine HPγCD DTG due to the incorporation of chitosan (Figure S3a-ii). For pristine pectin, there are three steps of weight losses corresponding to the dehydration of water (until 120 °C), degradation of lateral chains (220 °C), and breakdown of the backbone of polymer (320 °C).[37] The incorporation of pectin slightly decreased the intensity of the DTG and induced the appearance of a shoulder at around 335 °C. This shoulder became more prominent for 2%Chit/2%Pect/30%CD NF (Figure S2b-ii) compared to that for 3%Chit/1%Pect/30%CD NF (Figure S2c-ii) due to a higher amount of pectin within the sample. As seen in Figure S3, the thermal treatment of the sample did not significantly change its thermogram profile.

Disintegration, Swelling, and Degradation Profiles. First, the disintegration profile of NF was investigated in water (Videos S1−S3) over a short time (∼10 s). Here, thermally untreated 3%Chit/30%CD NF rapidly disintegrated with the addition of water, with small remnants of sample (Figure 3a-i). On the other hand, it became stable and remained in water along with a hydrogel feature after thermal treatment (120 °C for 1 h) (Figure 3a-i). In addition to the FTIR findings, this observation also proved the formation of a more durable interaction type between HPγCD and chitosan after thermal treatment compared to the untreated one. For the thermally treated and pectin-incorporated NFs, a similar profile was observed, and 3%Chit/1%Pect/30%CD NF and 2%Chit/2% Pect/30%CD NF maintained their substrate feature in the water (Figure 3a-ii,iii). It is noteworthy to mention that the thermally untreated 3%Chit/1%Pect/30%CD NF was also in tendency to disintegrate in water (Figure 3a-ii). Even 3%Chit/1%Pect/30%CD NF (Video S2) disintegrated faster than 3% Chit/30%CD NF (Video S1), which can be due to the increased amount of hydrophilic functional groups such as carboxyl and hydroxyl in addition to amino within the sample matrix by the incorporation of pectin.[38,39] However, the thermally untreated 2%Chit/2%Pect/30%CD NF did not disintegrate immediately upon the addition of water and indicated higher stability compared to others (Figure 3a-iii and Video S3). This can be attributed to the greater number of ionic interactions that occurred in the case of the component ratio of 2:2 chitosan/pectin (%, w/v) when compared to that of 3:1 chitosan/pectin (%, w/v). In one of the related studies, Cabello et al. reported the effect of different chitosan:pectin ratios on the hydrophilicity of the membrane.[40] Our results are correlated with theirs in which they showed that the blend membrane with a content of 50:50 (w/w, chitosan:pectin) had the lowest water uptake and so hydrophilicity compared to that of others (100:00, 80:20, and 60:40). This was based on the higher number of ionic complex formations in the case of the 50:50 combination that reduced the channel hydrophilicity.[40]

The thermally treated samples subsequently underwent swelling and degradation tests in PBS (pH 7.4) and acetate (pH 5.4) buffers for a longer duration (24 h) (Figure 3b,c). It was observed that all NFs completely degraded in the given conditions of the acidic medium (pH 5.4); therefore, swelling and degradation profiles could only be depicted for the PBS medium. Here, a higher swelling percentage was observed in the case of 3%Chit/1%Pect/30%CD NF (1511.7 ± 108.3%) compared to that in the 3%Chit/30%CD one (1339.6 ± 89.8%) (Figure 3b). This can be once again attributed to the higher content of hydrophilic groups in the NF matrix increased by the addition of pectin.[38,39] The opposite trend in the case of 2%Chit/2%Pect/30%CD NF (1434.1 ± 76.5%) can be again due to the increased interactions between chitosan and pectin, reflecting the balance between the charges of polymers.[39,40] Thus, the matrix of 2%Chit/2%Pect/30%CD NF becomes slightly more compact and less hydrophilic compared to the 3%Chit/1%Pect/30%CD NF-based sample. Even so, both pectin-incorporated NF demonstrated a higher swelling ratio than 3%Chit/30%CD NF. This can be due to the higher gellable polymer content in the case of 3%Chit/1% Pect/30%CD NF- and 2%Chit/2%Pect/30%CD NF-based samples (∼11.8%, w/w) compared to that of 3%Chit/30%CD NF (∼9.1%, w/w). The statistical analysis revealed that the

https://doi.org/10.1021/acssuschemeng.2c00650
ACS Sustainable Chem. Eng. 2022, 10, 4758−4769

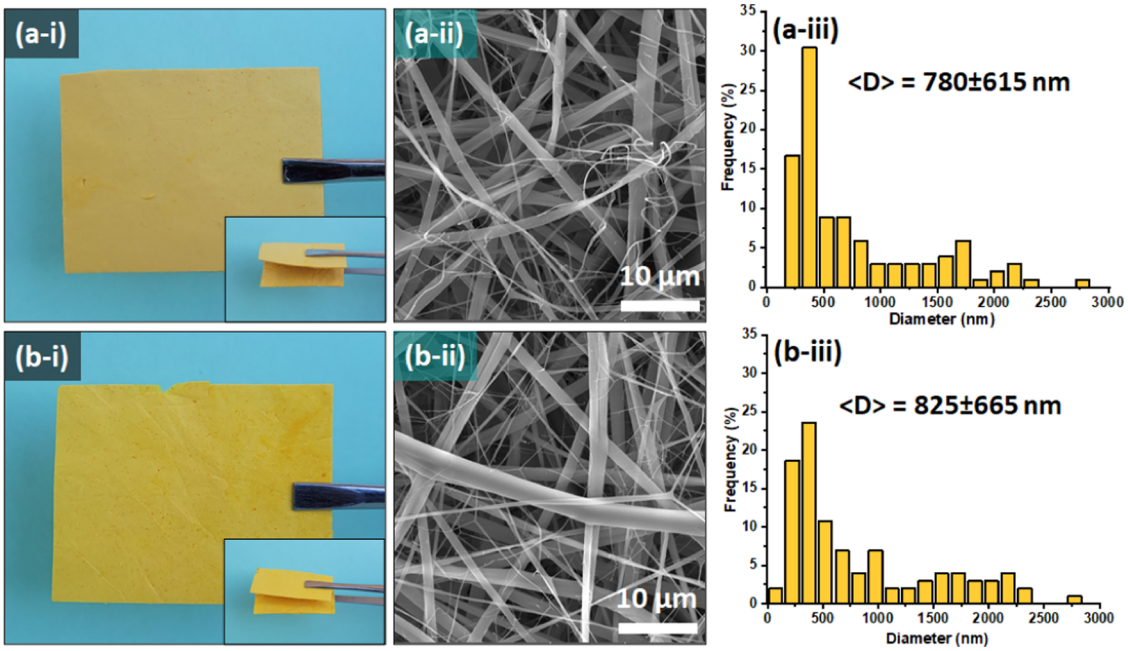

Figure 4. (i) Photos, (ii) SEM images, and (iii) diameter distributions of (a) 3%Chit/30%CD−Cur-IC NF and (b) 2%Chit/2%Pect/30%CD−Cur-IC NF.

mean swelling ratio of 3%Chit/30%CD NF and 3%Chit/1% Pect/30%CD NF is significantly different from each other ($p < 0.05$), while there is no significant difference between 3%Chit/30%CD NF and 2%Chit/2%Pect/30%CD NF ($p > 0.05$).

When the previous studies were inspected, Koosha et al.[41] and Sazegar et al.[42] reported ∼400 and ∼3356% swelling ratios for the electrospun NF of chitosan/poly(vinyl alcohol) (PVA) blends, respectively, which were cross-linked using different cross-linkers. On the other hand, Chee and co-workers claimed a 400−600% swelling ratio for the PVA/polyacrylic acid (PAA) bilayer NF.[43] In another study, Miranda et al. used the PVA/polyaniline (PANI) blend to produce hydrogel NF and reported a swelling ratio of ∼600%.[44] As observed, the swelling ratios that we found in our study are correlated with the previous ones in which highly hydrophilic polymer types were used to generate electrospun hydrogel-featured NFs and this suggested the hydrogel-forming capability of our samples.[41−44] For degradation tests in PBS buffer (pH 7.4), each sample independent of their compositions degraded ≥87% ($p < 0.05$: significantly different) (Figure 3c). The percentages for the thermally treated samples implied that the high concentration of HPγCD within the NF (∼88 to 91%, w/w) had the most influence on degradation of the samples due to a significantly high aqueous solubility of HPγCD (≥500 mg/mL).[45] On the other hand, the weakness of amine and carboxyl groups in acidic conditions can be a reason for the full degradation of nanofibrous films at pH 5.4.[46,47]

Characterization of Cyclodextrin−Curcumin Inclusion Complex (CD−Cur-IC). Figure S4a displays the XRD profiles of CD−Cur-IC, curcumin, and HPγCD powders. The XRD pattern of the CD−Cur physical mixture (PM) was also examined for comparison. The crystalline curcumin powder indicated distinctive diffraction peaks at 8.9 and 17.4°.[25] On the other hand, the hydroxypropylated CD is amorphous in structure; therefore, a broad halo XRD pattern was observed due to its nature.[22] The CD−Cur-IC powder possessed a similar amorphous XRD pattern with pure HPγCD, suggesting that curcumin was completely in the inclusion complex state. Despite the CD−Cur-PM having the same amount of curcumin as CD−Cur-IC, the crystalline peaks were obvious in the case of the physical mixture because of the uncomplexed state of curcumin (Figure S4a). The inclusion complex formation was further examined by DSC analysis. Here, DSC thermograms of curcumin indicated its crystalline nature by a melting peak at 177 °C. On the other hand, HPγCD did not show any melting peak due to its amorphous structure (Figure S4b). The endothermic peak at 30−140 °C corresponds to the dehydration of HPγCD molecules. For CD−Cur-IC powder, the melting peak of curcumin was not detected, validating the complete complex formation within the sample (Figure S4b). However, the melting peak of curcumin is rather obvious at the DSC thermogram of CD−Cur-PM (177 °C), proving the uncomplexed state of curcumin. Briefly, XRD and DSC findings are in good agreement with each other. The diffraction peaks and melting points can typically disappear in the case of inclusion complexes since guest molecules separated from each other cannot form the crystal structure over again.[48] CD−Cur-IC was prepared to have an initial molar ratio of 4:1 (CD/curcumin), which was found to be an efficient one for curcumin and HPγCD system in our previous study.[25] Here, ^{1}H-NMR measurements were conducted to determine the molar ratio between curcumin and HPγCD in CD−Cur-IC powder, and Figure S4c depicts the ^{1}H-NMR spectra of CD−Cur-IC, HPγCD, and curcumin. The molar ratio HPγCD:curcumin was determined as ∼4:1 from the integration of ^{1}H-NMR peaks. This finding revealed that curcumin was efficiently complexed with the HPγCD cavity by preserving the initial molar ratio during the whole process.

Characterization of CD−Cur-IC-Incorporated Nanofibrous Films. The electrospinning of CD−Cur-IC-included NF was carried out using the polymer concentrations of 3% chitosan (w/v) and 2% chitosan/2% pectin (w/v). The CD−Cur-IC was added to the electrospinning solution using the same concentration of 30% (w/v); therefore, samples are

https://doi.org/10.1021/acssuschemeng.2c00650
ACS Sustainable Chem. Eng. 2022, 10, 4758−4769

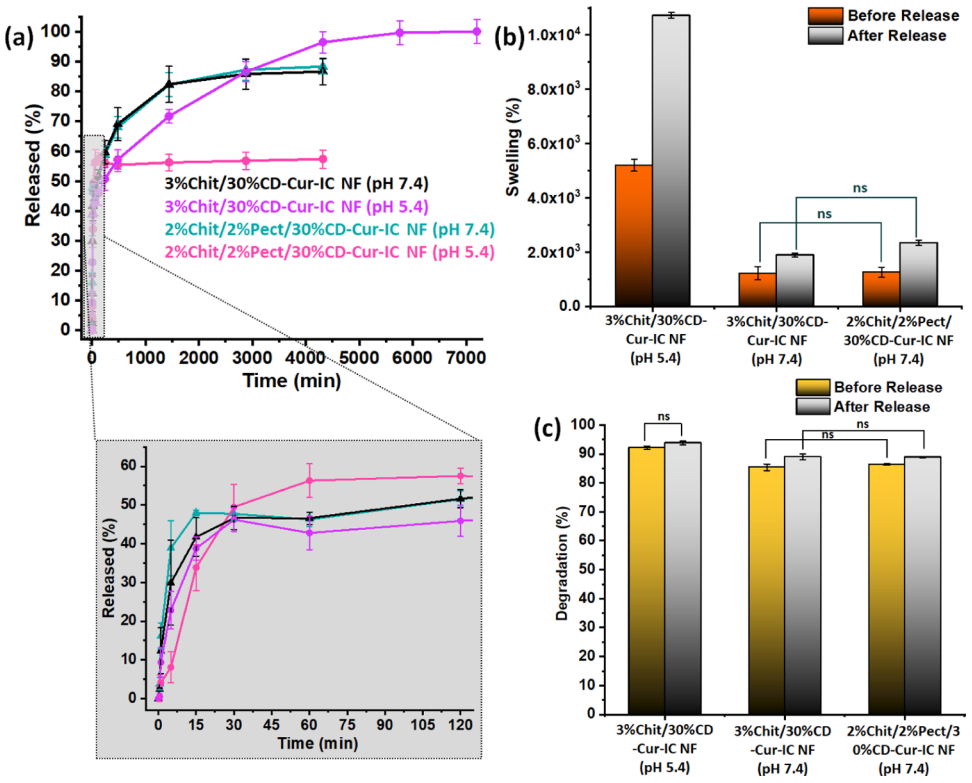

Figure 5. (a) Full and expanded *in vitro* release profiles of 3%Chit/30%CD−Cur-IC NF and 2%Chit/2%Pect/30%CD−Cur-IC NF in a liquid medium having pH values of 7.4 and 5.4. (b) Swelling and (c) degradation profiles of 3%Chit/30%CD−Cur-IC NF and 2%Chit/2%Pect/30% CD−Cur-IC NF before and after release tests (samples labeled with ns: $p > 0.05$; there is no significant difference).

called as 3%Chit/30%CD−Cur-IC NF and 2%Chit/2%Pect/30%CD−Cur-IC NF. Here, 2% chitosan/2% pectin blend having a higher amount of pectin compared to 3% chitosan/1% pectin was chosen as the control system to investigate the potential difference that might occur during release performance more apparently. Additionally, the proximate swelling/degradation values of 2%Chit/2%Pect/30%CD NF and 3% Chit/30%CD NF are the other reasons to be preferred for further study (Figure 3b,c). The electrospinning of 3%Chit/30%CD−Cur-IC NF and 2%Chit/2%Pect/30%CD−Cur-IC NF also yielded freestanding and flexible nanofibrous films (Figure 4a,b-i). Differently from the HPγCD-included samples, CD−Cur-IC-incorporated NF exhibited a yellow hue due to the characteristic color of curcumin. SEM imaging revealed the defect-free fiber morphology of 3%Chit/30%CD−Cur-IC NF and 2%Chit/2%Pect/30%CD−Cur-IC NF having AFDs of 780 ± 615 and 825 ± 665 nm, respectively (Figure 4a,b-ii,iii). According to statistical analysis, the difference of the mean diameter values is not significant ($p > 0.05$). The electrospinning of 3%Chit/30%CD−Cur-PM and 2%Chit/2%Pect/30%CD−Cur-PM was also performed for comparison. Here, the crystalline curcumin powder was physically mixed with the 3% chitosan/30% HPγCD (w/v) and 2% chitosan/2% pectin/30% HPγCD (w/v) solutions; however, it could not be homogeneously dispersed in the electrospinning system because of its poor solubility. Consequently, the electrospinning process was terribly affected by this incorporation such that inconsistent fibers and splashed areas were generated on the collector, which could not be peeled from the Al foil as a freestanding substrate (Figure S5). This finding revealed the importance of inclusion complex structures to sustain the stability during the electrospinning and so the formation of uniform and freestanding NF.

FTIR analysis was further conducted to ascertain the existence of curcumin and inclusion complex formation in the NF. Figure S6 displays the FTIR spectra of both pure HPγCD and CD−Cur-IC-incorporated samples. Curcumin has distinct peaks at 1625, 1601, 1505, and 1427 cm^{-1} corresponding to C═O stretching, aromatic C═C stretching, benzene ring vibration, and in-plane O−H deformation, respectively (Figure S6).[49] The same absorption bands are also obvious at the FTIR spectra of 3%Chit/30%CD−Cur-IC NF and 2%Chit/2%Pect/30%CD−Cur-IC NF. This result confirmed the loading of curcumin in the electrospun NF. Curcumin and HPγCD form inclusion complexes by the encapsulation of benzene rings of curcumin molecules into HPγCD cavities.[26] The hydrogen bonds, van der Waals forces, and/or hydrophobic interactions occurring during this complexation can cause wavenumber shifts of the curcumin characteristic peaks.[48] Our results indicated that there is a shift at the given peaks of curcumin from 1625, 1601, 1505, and 1427 cm^{-1} to 1628, 1603, 1513, and 1429 cm^{-1}, respectively. The relevant peaks belong to the benzene moiety of curcumin molecules, so the shifts observed in this region proved the inclusion complex formation between HPγCD and curcumin upon the entry of aromatic rings into the HPγCD cavity in the NFs (Figure S6).

***In Vitro* Release, Swelling, and Degradation Profiles.** In this study, the loading efficiencies of 3%Chit/30%CD−Cur-IC NF and 2%Chit/2%Pect/30%CD−Cur-IC NF were, respectively, determined as 88.1 ± 0.4 and 88.5 ± 1.9%. The curcumin release from electrospun NF at a temperature of 37 °C in the PBS (pH 7.4) and acetate (pH 5.4) buffer solutions

https://doi.org/10.1021/acssuschemeng.2c00650
ACS Sustainable Chem. Eng. 2022, 10, 4758−4769

is shown in Figure 5a. In the first 30 min, the cumulative release at pH 7.4 reached 46.6 ± 2.9 and 47.7 ± 1.8% for 3% Chit/30%CD−Cur-IC NF and 2%Chit/2%Pect/30%CD−Cur-IC NF, respectively. At pH 5.4, approximate release percentages of 46.2 ± 3.1 and 49.5 ± 5.8% were detected for 3%Chit/30%CD−Cur-IC NF and 2%Chit/2%Pect/30%CD−Cur-IC NF, respectively. It is obvious that there is no significant variation between the release rate of samples till 30 min; however, the release profile started to differentiate beyond this time point (Figure 5a). All the same, the release profile of these two NFs was almost identical to each other throughout the rest of the test for the pH 7.4 environment. Ultimately, 86.6 ± 4.4 and 88.4 ± 2.4% cumulative releases were achieved for 3%Chit/30%CD−Cur-IC NF and 2%Chit/2%Pect/30%CD−Cur-IC NF, respectively, after 3 days. On the other hand, the curcumin release percentage was found to be 56.2 ± 4.3% after 1 h from 2%Chit/2%Pect/30%CD−Cur-IC NF under acidic conditions (pH 5.4) (Figure 5a). Here, 2% Chit/2%Pect/30%CD−Cur-IC NF became swollen and then disintegrated into tiny pieces in the acidic medium in 1 h, and the release depicted a plateau profile from 1 h to the end of the test (3 days). In comparison with the burst release profile of curcumin from 2%Chit/2%Pect/30%CD−Cur-IC NF in pH 5.4, 3%Chit/30%CD−Cur-IC NF indicated a slower and higher release of curcumin, which eventuated in 100.1 ± 3.9% in the same medium by 5 days. The statistical analysis indicated that the release profile of 2%Chit/2%Pect/30%CD−Cur-IC NF in pH 5.4 is significantly different from that in pH 7.4 and also from the release profile of 3%Chit/30%CD−Cur-IC NF in pH 7.4 ($p < 0.05$).

Here, the swelling profile of NFs was investigated before and after the release test (Figure 5b). The swelling ratios of 3% Chit/30%CD−Cur-IC NF and 2%Chit/2%Pect/30%CD−Cur-IC NF before the release test were determined as 1220.4 ± 246.9 and 1257.2 ± 190.7%, respectively, in the PBS buffer (pH 7.4). After the release test, the values were detected as 1892.5 ± 78.2 and 2343.2 ± 95.1% for 3%Chit/30%CD−Cur-IC NF and 2%Chit/2%Pect/30%CD−Cur-IC NF, respectively. Nevertheless, the degradation percentages of CD−Cur-IC-included samples before (∼86% (w/w)) and after (∼89% (w/w)) release tests in the PBS buffer are similar to the HPγCD-included ones (≥88% (w/w)) (Figure 5c). Even so, a similar trend was observed, where the 2%Chit/2%Pect/30% CD-based system had a relatively higher swelling ratio compared to the 3%Chit/30%CD-based one. The difference between the swelling ratios of samples became more apparent, especially after the release tests in which higher swelling ratios were observed compared to those detected at swelling analysis. However, this difference between the swelling ratio did not influence the release of curcumin, and 3%Chit/30%CD−Cur-IC NF and 2%Chit/2%Pect/30%CD−Cur-IC NF showed an identical release profile in pH 7.4 medium where an initial burst release had arisen within the first 30 min, followed by a sustained release before reaching a plateau after 2 days (Figure 5a).

Unlike 2%Chit/2%Pect/30%CD−Cur-IC NF, 3%Chit/30% CD−Cur-IC NF became swollen and protected its substrate integrity in pH 5.4 medium. Therefore, we were able to determine both swelling and degradation profiles of 3%Chit/30%CD−Cur-IC NF before and subsequent to the release test conducted in acetate medium (pH 5.4). Here, the swelling and degradation ratios were, respectively, detected as 5202.9 ± 218.8 and ∼92% (w/w) before the release test and 10725.8 ± 97.9 and ∼93% (w/w) after the release test for 3%Chit/30% CD−Cur-IC NF (Figure 5b,c). The dramatically high swelling ratio of 3%Chit/30%CD−Cur-IC NF in acetate buffer was due to the protonation of chitosan chains under acidic conditions. This led to the expansion of polymer chains by the electrostatic repulsion, so the NFs swelled to a larger extent by absorbing a higher amount of liquid medium, and this also promoted curcumin release (Figure 5a).[50] As mentioned previously, the weakness of amine and carboxyl groups in acidic conditions could render these samples more tender in pH 5.4 medium compared to that in pH 7.4 one. Here, the degradation of 2% Chit/2%Pect/30%CD−Cur-IC NF in ∼1 h or the extremely high swelling profile of 3%Chit/30%CD−Cur-IC NF can be attributed to this action. Besides, the better stability of 3% Chit/30%CD−Cur-IC NF in the acetate medium can be attached to the absence of pectin, which increases the intensity of carboxyl groups within the sample structure. It is also noteworthy to mention that the varied swelling ratios and degradation profiles of nanofibrous films compared to those of previously analyzed 3%Chit/30%CD NF- and 2%Chit/2% Pect/30%CD NF-based samples can be due to the inclusion complex state of HPγCD. The higher swelling ratios of Cur-CD-IC-incorporated NF detected after the release test compared to those of swelling tests (1 day) are unsurprisingly due to the longer duration of testing.

The release behavior of NF was further examined by fitting release data to five different kinetic models (zero-order, first-order, Higuchi, Korsmeyer−Peppas, and Hixson−Crowell). The applied formulations and the correlation coefficients (R^2) are summarized in the Supporting Information (Table S2). As indicated in Table S2, the release kinetics of samples did not fit with the zero-order kinetics in both buffer medium having pH values 5.4 and 7.4. Except for the release profile of 2%Chit/2% Pect/30%CD−Cur-IC NF at pH 5.4, the comparison of R^2 values depicted that the curcumin release can be much better described by first-order and Higuchi models compared to that of the zero-order model, suggesting the diffusion-controlled release in a time-dependent manner (Fick's first law).[51,52] Here, it is noteworthy to state that the highest R^2 value (0.9485) was obtained for 3%Chit/30%CD−Cur-IC NF at pH 5.4, confirming the more sustained release of curcumin compared to other release cases. On the other hand, relatively higher R^2 was found with the Korsmeyer−Peppas model compared to that with other models for 2%Chit/2%Pect/30% CD−Cur-IC NF at pH 5.4. This confirmed the erosion-controlled release of curcumin from this sample where the progressive disappearance occurred after 1 h in the aqueous medium. For the Korsmeyer−Peppas model, all R^2 values approximated each other. This finding established that the erosion/diffusion-based release behavior is somehow influential for all cases, and this matched with degradation study results. Additionally, diffusion exponent (n) values determined <0.45 for all cases, suggesting the dominant mechanism of Fickian diffusion (Table S2).[51−53] Here, the release kinetic of curcumin from 3%Chit/30%CD−Cur-IC NF at pH 5.4 can also be described by Hixson−Crowell with an R^2 value of 0.9574. The Hixson−Crowell model is related to the change in the surface area with the progressive disintegration of matrix as a function of time.[54] This confirmed the swelling and degradation behavior of 3%Chit/30%CD−Cur-IC NF in the acetate medium in a progressing time, which gave rise to more curcumin release in a further controlled manner. According to all of these findings, it can be said that the curcumin release

https://doi.org/10.1021/acssuschemeng.2c00650
ACS Sustainable Chem. Eng. 2022, 10, 4758−4769

from the NF of the CD-IC-incorporated chitosan/pectin blend system can be achieved in a pH-responsive manner. Here, the drug release of curcumin was tested at both pH 5.4 and pH 7.4 to simulate the microenvironment of normal skin and wound. The variety of release profiles can be associated with the swelling behavior of nanofibrous films at different pH values, and this can meet the needs during the different stages of the wound healing process. Additionally, as it is known, maintaining the body fluid, wound exudates, and metabolites are crucial features of wound dressing patches.[55] Therefore, the hydrogel-forming capacity of our sample by swelling in high % can also suggest the acceptable efficiency for the absorption of wound exudate during the treatments.

CONCLUSIONS

Electrospinning technique can offer a green way to develop functional nanofibrous films of biopolymers derived from natural sources. In this study, the most abundantly found polysaccharide types of chitosan and pectin were rendered into freestanding and flexible nanofibrous films due to the incorporation of cyclodextrin (CD) molecules. For this purpose, highly water-soluble hydroxypropyl-γ-cyclodextrin (HPγCD) (30%, w/v) was mixed with different ratios of chitosan/pectin blends (3/0, 3/1, and 2/2%, w/v), and this enabled and facilitated the fiber formation from these sustainable biopolymers. Here, it was detected that the increased viscosity and decreased conductivity values of the electrospinning solutions by the incorporation of CD enabled the generation of uniform fibers during the process. The altered chitosan/pectin ratio resulted in different disintegration behaviors in the aqueous medium depending on the strength of the polyelectrolyte complex formed between the polar functional groups of chitosan and pectin. However, the stability of nanofibrous films in the aqueous medium was enhanced by a mild thermal treatment (1 h at 120 °C) and they gained hydrogel-forming capability in a particular pH environment by different swelling ratios (%). Using CD as the carrier matrix during the electrospinning process accompanied several advantages unlike the common way of using the polymeric matrix. First, there was no need for toxic organic solvents to prepare the electrospinning solutions, and the GRAS solvent of acetic acid was used to dissolve all components. Second, the concentration of CD (30%, w/v) applied for the process enabled the production of nanofibrous films with a higher deposition efficiency compared to that of the polymeric system in which the electrospinning solutions are usually prepared using lower solid polymer contents (3−15%, w/v). Above all, the unique inclusion complexation feature of CD made possible further encapsulation of curcumin within the nanofibrous films without disturbing the fiber formation process and by ensuring an enhanced aqueous solubility for this non-water-soluble bioactive compound. Here, the CD−curcumin inclusion complex (CD−Cur-IC) powder produced with a molar ratio of 4:1 (CD/guest) was incorporated into chitosan/pectin solutions having the predetermined blend ratios (3/0 and 2/2%, w/v). The freestanding and homogeneous nanofibrous films were obtained with an ∼89% loading efficiency of curcumin. The *in vitro* release tests conducted in two different pH values representing the microenvironments of normal skin (pH 5.4) and wound (pH 7.4) demonstrated the pH-responsive release potential of nanofibrous films. Here, the varied compositions and so the swelling ratios of nanofibrous films provided different release profiles from burst to sustained, which might be attractive for the various phases of wound healing. Briefly, the nanofibrous films generated by a green process, in which the renewable biopolymers of chitosan and pectin and the nontoxic starch-derived product of CD were used, might hold a high potential as a new-generation biomaterial. In this way, biopolymers extracted from the residuals of industrial activities can be utilized for the development of high-valued products. This sustainable approach can be another step contributing to the elimination of environmental and health loadings raised from the use of petroleum-based products.

ASSOCIATED CONTENT

Supporting Information

The Supporting Information is available free of charge at https://pubs.acs.org/doi/10.1021/acssuschemeng.2c00650.

Structural characterization data of nanofibrous films (TGA and FTIR) and CD−Cur-IC powder (XRD, DSC, and ^{1}H-NMR); additional optical microscopy images and photos of samples; and release kinetic calculations and results (PDF)

Disintegration profile of 3%Chit/30%CD NF before and after thermal treatment (Video_S1) (MP4)

Disintegration profile of 3%Chit/1%Pect/30%CD NF before and after thermal treatment (Video_S2) (MP4)

Disintegration profile of 2%Chit/2%Pect/30%CD NF before and after thermal treatment (Video_S3) (MP4)

AUTHOR INFORMATION

Corresponding Authors

Asli Celebioglu − *Fiber Science Program, Department of Human Centered Design, College of Human Ecology, Cornell University, Ithaca, New York 14853, United States;* orcid.org/0000-0002-5563-5746; Email: ac2873@cornell.edu

Tamer Uyar − *Fiber Science Program, Department of Human Centered Design, College of Human Ecology, Cornell University, Ithaca, New York 14853, United States;* orcid.org/0000-0002-3989-4481; Email: tu46@cornell.edu

Author

Antonio Frank Saporito − *Department of Chemistry and Chemical Biology, Cornell University, Ithaca, New York 14853, United States*

Complete contact information is available at: https://pubs.acs.org/10.1021/acssuschemeng.2c00650

Author Contributions

A.C. performed conceptualization, methodology, investigation, and writing of the original draft. A.F.S. performed investigation and writing of the original draft. T.U. supervised the study and participated in conceptualization, methodology, editing the final version, funding acquisition, and project administration of the study.

Notes

The authors declare no competing financial interest.

ACKNOWLEDGMENTS

This work made use of the Cornell Center for Materials Research Shared Facilities, which were supported through the NSF MRSEC program (DMR-1719875), the Cornell Chem-

istry NMR Facility supported in part by the NSF MRI program (CHE-1531632), and the Department of Human Centered Design facilities.

REFERENCES

(1) Rosenboom, J.-G.; Langer, R.; Traverso, G. Bioplastics for a Circular Economy. *Nat. Rev. Mater.* **2022**, *7*, 117−137.
(2) Gironi, F.; Piemonte, V. Bioplastics and Petroleum-Based Plastics: Strengths and Weaknesses. *Energy Sources, Part A* **2011**, *33*, 1949−1959.
(3) Rai, P.; Mehrotra, S.; Priya, S.; Gnansounou, E.; Sharma, S. K. Recent Advances in the Sustainable Design and Applications of Biodegradable Polymers. *Bioresour. Technol.* **2021**, *325*, No. 124739.
(4) Akshaykumar, K. P.; Zare, E. N.; Torres-Mendieta, R.; Wacławek, S.; Makvandi, P.; Černík, M.; Padil, V. V. T.; Varma, R. S. Electrospun Fibers Based on Botanical, Seaweed, Microbial, and Animal Sourced Biomacromolecules and Their Multidimensional Applications. *Int. J. Biol. Macromol.* **2021**, *171*, 130−149.
(5) Kou, S. G.; Peters, L.; Mucalo, M. Chitosan: A Review of Molecular Structure, Bioactivities and Interactions with the Human Body and Micro-Organisms. *Carbohydr. Polym.* **2022**, *282*, No. 119132.
(6) Li, D.; Li, J.; Dong, H.; Li, X.; Zhang, J.; Ramaswamy, S.; Xu, F. Pectin in Biomedical and Drug Delivery Applications: A Review. *Int. J. Biol. Macromol.* **2021**, *185*, 49−65.
(7) Li, Y.; Wang, J.; Wang, Y.; Cui, W. Advanced Electrospun Hydrogel Fibers for Wound Healing. *Composites, Part B* **2021**, *223*, No. 109101.
(8) Grewal, M. G.; Highley, C. B. Electrospun Hydrogels for Dynamic Culture Systems: Advantages, Progress, and Opportunities. *Biomater. Sci.* **2021**, *9*, 4228−4245.
(9) Xue, J.; Wu, T.; Dai, Y.; Xia, Y. Electrospinning and Electrospun Nanofibers: Methods, Materials, and Applications. *Chem. Rev.* **2019**, *119*, 5298−5415.
(10) Aytac, Z.; Huang, R.; Vaze, N.; Xu, T.; Eitzer, B. D.; Krol, W.; MacQueen, L. A.; Chang, H.; Bousfield, D. W.; Chan-Park, M. B.; et al. Development of Biodegradable and Antimicrobial Electrospun Zein Fibers for Food Packaging. *ACS Sustainable Chem. Eng.* **2020**, *8*, 15354−15365.
(11) Xu, T.; Ma, C.; Aytac, Z.; Hu, X.; Ng, K. W.; White, J. C.; Demokritou, P. Enhancing Agrichemical Delivery and Seedling Development with Biodegradable, Tunable, Biopolymer-Based Nanofiber Seed Coatings. *ACS Sustainable Chem. Eng.* **2020**, *8*, 9537−9548.
(12) Yi, S.; Wu, Y.; Zhang, Y.; Zou, Y.; Dai, F.; Si, Y. Antibacterial Activity of Photoactive Silk Fibroin/Cellulose Acetate Blend Nanofibrous Membranes against Escherichia Coli. *ACS Sustainable Chem. Eng.* **2020**, *8*, 16775−16780.
(13) Hsiung, E.; Celebioglu, A.; Chowdhury, R.; Kilic, M. E.; Durgun, E.; Altier, C.; Uyar, T. Antibacterial Nanofibers of Pullulan/Tetracycline-Cyclodextrin Inclusion Complexes for Fast-Disintegrating Oral Drug Delivery. *J. Colloid Interface Sci.* **2022**, *610*, 321−333.
(14) Qasim, S. B.; Zafar, M. S.; Najeeb, S.; Khurshid, Z.; Shah, A. H.; Husain, S.; Rehman, I. U. Electrospinning of Chitosan-Based Solutions for Tissue Engineering and Regenerative Medicine. *Int. J. Mol. Sci.* **2018**, *19*, 407.
(15) Anisiei, A.; Oancea, F.; Marin, L. Electrospinning of Chitosan-Based Nanofibers: From Design to Prospective Applications. *Rev. Chem. Eng.* **2020**.
(16) Iacob, A.-T.; Drăgan, M.; Ionescu, O.-M.; Profire, L.; Ficai, A.; Andronescu, E.; Confederat, L. G.; Lupaşcu, D. An Overview of Biopolymeric Electrospun Nanofibers Based on Polysaccharides for Wound Healing Management. *Pharmaceutics* **2020**, *12*, 983.
(17) Ignatova, M.; Manolova, N.; Rashkov, I. Electrospun Antibacterial Chitosan-Based Fibers. *Macromol. Biosci.* **2013**, *13*, 860−872.
(18) Ohkawa, K.; Cha, D.; Kim, H.; Nishida, A.; Yamamoto, H. Electrospinning of Chitosan. *Macromol. Rapid Commun.* **2004**, *25*, 1600−1605.
(19) Burns, N. A.; Burroughs, M. C.; Gracz, H.; Pritchard, C. Q.; Brozena, A. H.; Willoughby, J.; Khan, S. A. Cyclodextrin Facilitated Electrospun Chitosan Nanofibers. *RSC Adv.* **2015**, *5*, 7131−7137.
(20) Carneiro, S. B.; Duarte, C.; Ílary, F.; Heimfarth, L.; Quintans, S.; de Souza, J.; Quintans-Júnior, L. J.; Veiga Júnior, V. F.; da Neves; de Lima, ÁA.; et al. Cyclodextrin−Drug Inclusion Complexes: In Vivo and In Vitro Approaches. *Int. J. Mol. Sci.* **2019**, *20*, 642.
(21) Crini, G. A History of Cyclodextrins. *Chem. Rev.* **2014**, *114*, 10940−10975.
(22) Celebioglu, A.; Uyar, T. Electrospinning of Nanofibers from Non-Polymeric Systems: Polymer-Free Nanofibers from Cyclodextrin Derivatives. *Nanoscale* **2012**, *4*, 621−631.
(23) Celebioglu, A.; Uyar, T. Electrospinning of Cyclodextrins: Hydroxypropyl-Alpha-Cyclodextrin Nanofibers. *J. Mater. Sci.* **2020**, *55*, 404−420.
(24) Celebioglu, A.; Wang, N.; Kilic, M. E.; Durgun, E.; Uyar, T. Orally Fast Disintegrating Cyclodextrin/Prednisolone Inclusion-Complex Nanofibrous Webs for Potential Steroid Medications. *Mol. Pharm.* **2021**, *18*, 4486−4500.
(25) Celebioglu, A.; Uyar, T. Fast-Dissolving Antioxidant Curcumin/Cyclodextrin Inclusion Complex Electrospun Nanofibrous Webs. *Food Chem.* **2020**, *317*, No. 126397.
(26) Celebioglu, A.; Uyar, T. Hydrocortisone/Cyclodextrin Complex Electrospun Nanofibers for a Fast-Dissolving Oral Drug Delivery System. *RSC Med. Chem.* **2020**, *11*, 245−258.
(27) Celebioglu, A.; Uyar, T. Electrospinning of Polymer-Free Nanofibers from Cyclodextrin Inclusion Complexes. *Langmuir* **2011**, *27*, 6218−6226.
(28) Braga, S. S. Cyclodextrins: Emerging Medicines of the New Millennium. *Biomolecules* **2019**, *9*, 801.
(29) Rauf, A.; Imran, M.; Orhan, I. E.; Bawazeer, S. Health Perspectives of a Bioactive Compound Curcumin: A Review. *Trends Food Sci. Technol.* **2018**, *74*, 33−45.
(30) Uyar, T.; Besenbacher, F. Electrospinning of Uniform Polystyrene Fibers: The Effect of Solvent Conductivity. *Polymer* **2008**, *49*, 5336−5343.
(31) Khatun, B.; Baishya, P.; Ramteke, A.; Maji, T. K. Study of the Complexation of Structurally Modified Curcumin with Hydroxypropyl Beta Cyclodextrin and Its Effect on Anticancer Activity. *New J. Chem.* **2020**, *44*, 4887−4897.
(32) Maciel, V. B. V.; Yoshida, C. M. P.; Franco, T. T. Chitosan/Pectin Polyelectrolyte Complex as a PH Indicator. *Carbohydr. Polym.* **2015**, *132*, 537−545.
(33) Tripathi, S.; Mehrotra, G. K.; Dutta, P. K. Preparation and Physicochemical Evaluation of Chitosan/Poly (Vinyl Alcohol)/Pectin Ternary Film for Food-Packaging Applications. *Carbohydr. Polym.* **2010**, *79*, 711−716.
(34) Garnica-Palafox, I. M.; Sánchez-Arévalo, F. M. Influence of Natural and Synthetic Crosslinking Reagents on the Structural and Mechanical Properties of Chitosan-Based Hybrid Hydrogels. *Carbohydr. Polym.* **2016**, *151*, 1073−1081.
(35) Bernabé, P.; Peniche, C.; Argüelles-Monal, W. Swelling Behavior of Chitosan/Pectin Polyelectrolyte Complex Membranes. Effect of Thermal Cross-Linking. *Polym. Bull.* **2005**, *55*, 367−375.
(36) Soubhagya, A. S.; Moorthi, A.; Prabaharan, M. Preparation and Characterization of Chitosan/Pectin/ZnO Porous Films for Wound Healing. *Int. J. Biol. Macromol.* **2020**, *157*, 135−145.
(37) C, M.; Kanmani, B. R.; Sharmila, G.; Kumar, M.; Shanmugaprakash, M. Carboxymethylation of Pectin: Optimization, Characterization and in-Vitro Drug Release Studies. *Carbohydr. Polym.* **2018**, *194*, 311−318.
(38) Demir, D.; Ceylan, S.; Göktürk, D.; Bölgen, N. Extraction of Pectin from Albedo of Lemon Peels for Preparation of Tissue Engineering Scaffolds. *Polym. Bull.* **2021**, *78*, 2211−2226.
(39) Shitrit, Y.; Davidovich-Pinhas, M.; Bianco-Peled, H. Shear Thinning Pectin Hydrogels Physically Cross-Linked with Chitosan Nanogels. *Carbohydr. Polym.* **2019**, *225*, No. 115249.
(40) Pasini Cabello, S.; Ochoa, N. A.; Takara, E. A.; Mollá, S.; Compañ, V. Influence of Pectin as a Green Polymer Electrolyte on the

https://doi.org/10.1021/acssuschemeng.2c00650
ACS Sustainable Chem. Eng. 2022, 10, 4758−4769

Transport Properties of Chitosan-Pectin Membranes. *Carbohydr. Polym.* **2017**, *157*, 1759−1768.
(41) Koosha, M.; Raoufi, M.; Moravvej, H. One-Pot Reactive Electrospinning of Chitosan/PVA Hydrogel Nanofibers Reinforced by Halloysite Nanotubes with Enhanced Fibroblast Cell Attachment for Skin Tissue Regeneration. *Colloids Surf., B* **2019**, *179*, 270−279.
(42) Sazegar, M.; Bazgir, S.; Katbab, A. A. Preparation and Characterization of Water-Absorbing Gas-Assisted Electrospun Nanofibers Based on Poly (Vinyl Alcohol)/Chitosan. *Mater. Today Commun.* **2020**, *25*, No. 101489.
(43) Chee, B. S.; de Lima, G. G.; de Lima, T. A. M.; Seba, V.; Lemarquis, C.; Pereira, B. L.; Bandeira, M.; Cao, Z.; Nugent, M. Effect of Thermal Annealing on a Bilayer Polyvinyl Alcohol/Polyacrylic Acid Electrospun Hydrogel Nanofibres Loaded with Doxorubicin and Clarithromycin for a Synergism Effect against Osteosarcoma Cells. *Mater. Today Chem.* **2021**, *22*, No. 100549.
(44) Miranda, D. O.; Dorneles, M. F.; Oréfice, R. L. One-Step Process for the Preparation of Fast-Response Soft Actuators Based on Electrospun Hybrid Hydrogel Nanofibers Obtained by Reactive Electrospinning with in Situ Synthesis of Conjugated Polymers. *Polymer* **2020**, *200*, No. 122590.
(45) Kim, D.-H.; Lee, S.-E.; Pyo, Y.-C.; Tran, P.; Park, J.-S. Solubility Enhancement and Application of Cyclodextrins in Local Drug Delivery. *J. Pharm. Invest.* **2020**, *50*, 17−27.
(46) Abasalta, M.; Asefnejad, A.; Khorasani, M. T.; Saadatabadi, A. R.; Irani, M. Adsorption and Sustained Release of Doxorubicin from N-Carboxymethyl Chitosan/Polyvinyl Alcohol/Poly (ε-Caprolactone) Composite and Core-Shell Nanofibers. *J. Drug Delivery Sci. Technol.* **2021**, *67*, No. 102937.
(47) Abid, S.; Hussain, T.; Nazir, A.; Zahir, A.; Ramakrishna, S.; Hameed, M.; Khenoussi, N. Enhanced Antibacterial Activity of PEO-Chitosan Nanofibers with Potential Application in Burn Infection Management. *Int. J. Biol. Macromol.* **2019**, *135*, 1222−1236.
(48) Narayanan, G.; Boy, R.; Gupta, B. S.; Tonelli, A. E. Analytical Techniques for Characterizing Cyclodextrins and Their Inclusion Complexes with Large and Small Molecular Weight Guest Molecules. *Polym. Test.* **2017**, *62*, 402−439.
(49) Gumireddy, A.; Christman, R.; Kumari, D.; Tiwari, A.; North, E. J.; Chauhan, H. Preparation, Characterization, and In Vitro Evaluation of Curcumin-and Resveratrol-Loaded Solid Lipid Nanoparticles. *AAPS PharmSciTech* **2019**, *20*, No. 145.
(50) Guo, H.; Tan, S.; Gao, J.; Wang, L. Sequential Release of Drugs Form a Dual-Delivery System Based on PH-Responsive Nanofibrous Mats towards Wound Care. *J. Mater. Chem. B* **2020**, *8*, 1759−1770.
(51) Peppas, N. A.; Narasimhan, B. Mathematical Models in Drug Delivery: How Modeling Has Shaped the Way We Design New Drug Delivery Systems. *J. Controlled Release* **2014**, *190*, 75−81.
(52) Chen, M.; Li, L.; Xia, L.; Jiang, S.; Kong, Y.; Chen, X.; Wang, H. The Kinetics and Release Behaviour of Curcumin Loaded PH-Responsive PLGA/Chitosan Fibers with Antitumor Activity against HT-29 Cells. *Carbohydr. Polym.* **2021**, *265*, No. 118077.
(53) Kersani, D.; Mougin, J.; Lopez, M.; Degoutin, S.; Tabary, N.; Cazaux, F.; Janus, L.; Maton, M.; Chai, F.; Sobocinski, J.; Blanchemain, N.; Martel, B. Stent Coating by Electrospinning with Chitosan/Poly-Cyclodextrin Based Nanofibers Loaded with Simvastatin for Restenosis Prevention. *Eur. J. Pharm. Biopharm.* **2020**, *150*, 156−167.
(54) Gouda, R.; Baishya, H.; Qing, Z. Application of Mathematical Models in Drug Release Kinetics of Carbidopa and Levodopa ER Tablets. *J. Dev. Drugs* **2017**, *6*, No. 1000171.
(55) Alven, S.; Aderibigbe, B. A. Fabrication of Hybrid Nanofibers from Biopolymers and Poly (Vinyl Alcohol)/Poly (ε-Caprolactone) for Wound Dressing Applications. *Polymers* **2021**, *13*, 2104.

https://doi.org/10.1021/acssuschemeng.2c00650
ACS Sustainable Chem. Eng. 2022, 10, 4758−4769